JOURNAL OF CATALYSIS **179,** 515–527 (1998)
ARTICLE NO. CA982252

Copper- and Silver–Zirconia Aerogels: Preparation, Structural Properties and Catalytic Behavior in Methanol Synthesis from Carbon Dioxide

René A. Köppel, Carsten Stöcker, and Alfons Baiker[1]

Laboratory of Technical Chemistry, Swiss Federal Institute of Technology, ETH-Zentrum, CH-8092 Zürich, Switzerland

Received March 31, 1998; revised June 10, 1998; accepted July 17, 1998

Copper- and silver-zirconia aerogels containing 10 at% IB metal were prepared from tetra-*n*-butoxy zirconium(IV) and IB metal acetates using the solution sol-gel method and ensuing high-temperature (HT) and low-temperature (LT) supercritical drying, respectively. The influence of preparation parameters and calcination on the structural and catalytic properties of the aerogels for the synthesis of methanol from carbon dioxide and hydrogen was investigated. After calcination in air at 573 K, the catalysts had BET surface areas in the range of 100–143 $m^2 \cdot g^{-1}$ (Cu/ZrO_2) and 77–125 $m^2 \cdot g^{-1}$ (Ag/ZrO_2), respectively. Due to the reductive alcoholic atmosphere during high-temperature supercritical drying, metallic copper and silver existed in all raw HT-aerogels. The mean size of the copper crystallites was 30 nm. The silver crystallite size for the HT-aerogel prepared with nitric acid was 10 nm, whereas for samples prepared with acetic acid it was 5–7 nm. Calcination in air at 573 K led to the formation of highly dispersed amorphous copper oxide and silver. Comparing the catalytic behavior of the calcined copper–zirconia aerogels with corresponding xerogels prepared by coprecipitation revealed highest activity for the LT-aerogel, whereas the HT-aerogels were least active. In contrast, similar catalytic behavior was observed for the differently dried silver-zirconia samples. Generally, CO_2-conversion of the copper–zirconia aerogels was markedly higher than that of the corresponding silver–zirconia aerogels, whereas methanol selectivity was similar.

Key Words: **sol-gel; aerogel; copper/zirconia; silver/zirconia; methanol synthesis; CO_2-hydrogenation.**

INTRODUCTION

The utilization of carbon dioxide as a starting material for the manufacture of valuable fuels and chemicals has gained considerable attention in view of the abundant availability of CO_2 (1–6). Several studies have been concerned with the use of CO_2 as a C1 building block for the production of methanol, hydrocarbons, amines, or formic acid and its derivatives (1–8). Methanol is currently produced on an industrial scale from syngas (CO, CO_2, and H_2) employing copper based catalysts (3). However, using CO_2 in place of CO for methanol synthesis remains an interesting challenge for CO_2 utilization (9).

Among the metal oxides tested as support materials for CO_2 hydrogenation catalysts, ZrO_2 is of special interest because of its mechanical and thermal stability, its high specific surface area, and its intrinsic catalytic properties (10–12). In recent studies covering transition metal–zirconia catalysts, copper–zirconia showed interesting properties for methanol synthesis from carbon dioxide (13–30), whereas silver exhibited surprisingly high selectivity to methanol, although activity was generally lower than observed for copper-containing catalysts (24, 25).

Various methods for preparing copper- or silver–zirconia catalysts for the synthesis of methanol from CO_2/H_2 have been reported, among which coprecipitation yielded most suitable catalysts (22, 25). It has been shown that the starting salt used for coprecipitation (26) and the nature of the precipitant (22, 31) strongly influence the behavior of the catalysts. Whereas precipitation with sodium- or ammonium-carbonate gave dense materials of low catalytic activity, gelatinous precipitates exhibiting high activity were obtained for preparations with NaOH as precipitant (22, 31). High dispersion of the metal constituent, resulting in a high metal-to-oxide interfacial contact area in the catalysts, was proposed to be crucial for high activity and selectivity in methanol synthesis (22, 25). Recently, sol-gel chemistry, combined with supercritical drying, has attracted considerable attention as an interesting method for the preparation of supported metal catalysts, since it may produce homogeneous materials of high dispersion and uniform distribution of the metal throughout the solid (17, 32–37). The potential of aerogels for catalysis resides in their unique morphological and chemical properties, which originate from their wet chemical preparation by the solution-sol-gel method and the subsequent removal of the solvent via supercritical drying. The advantages of the solution-sol-gel technique for catalyst preparation comprise molecular-scale mixing of the constituents, the control of the structure and composition at a molecular scale, and the purity of the precursors, which allows the preparation of materials without contamination

[1] To whom correspondence should be addressed. E-mail: baiker@tech.chem.ethz.ch.

0021-9517/98 $25.00

by, e.g., alkaline compounds as often found for coprecipitated catalysts.

Studies aiming at the preparation of zirconia based aerogels focussed on aspects of the preparation procedure and the drying variables. With respect to copper–zirconia aerogels different attempts for the preparation of the catalysts are reported, including impregnation of ZrO_2 aerogels with the copper precursor followed by conventional drying (38), impregnation of a zirconia aerogel with the copper precursor and ensuing high temperature supercritical drying (17, 39), and the coprecipitation of the copper and zirconium precursor with KOH followed by washing with ethanol and high temperature supercritical drying (40–42).

The aim of the present work was to prepare copper–zirconia and silver–zirconia aerogels with high surface area, which combine good metal dispersion with favorable textural properties. Sol-gel preparation was used to obtain catalysts free of alkaline contamination. The influence of preparation parameters, drying method, and calcination on the structural properties and the catalytic behavior in methanol synthesis from carbon dioxide was investigated.

EXPERIMENTAL

Sol-Gel Aerogel Preparation

Analytical grade reagents were used throughout this work. The sol-gel synthesis was carried out in an anti-adhesive, closed Teflon beaker under nitrogen atmosphere and at ambient temperature (297 ± 2 K). Details of the preparation are listed in Table 1.

One-stage preparation (os). Two different solutions were prepared. Solution A consisted of 41.25-g tetra-*n*-butoxy zirconium(IV) (80 wt% TBOZ in butanol), and 1.72 g copper or 1.44 g silver acetate, dissolved in 90-ml ethanol. Solution B (hydrolysant) contained doubly distilled water and 0.48 ml nitric acid (65 wt%) or 0.4 ml acetic acid, diluted in 36 ml ethanol. The corresponding molar ratios ($n_{H_2O} : n_{TBOZ} : n_{Acid}$) were 4 : 1 : 0.08. The amounts of metal precursors were adjusted to prepare catalysts with atomic IB metal-to-zirconium ratios of 0.1. After homogenization for 5 min, solution B was quickly added via a dropping funnel to solution A under stirring (ca 500 rpm). The resulting opaque gels (gelation time <1 min) were aged for 23 h and then redispersed with 100 ml ethanol using a glass rod.

Two-stage preparation (ts). In this case, solution A was made up only of TBOZ diluted in 60 ml ethanol. After mixing with solution B the sol-gel product was aged for 1 h. Subsequently, a solution of copper or silver acetate in 30-ml ethanol was added under vigorous stirring. The resulting gel was aged for 22 h and then redispersed in 100 ml ethanol.

High-temperature (HT) supercritical drying. Supercritical drying at high temperature was carried out following the procedure described in detail in Ref. (43). The sol-gel product was transferred into an autoclave. The high-pressure system was flushed with nitrogen, pressurized with 5 MPa nitrogen, hermetically closed, and heated at 1 K min^{-1} to 533 K. After thermal equilibration for 30 min the pressure (14 MPa) was isothermally released at 0.1 MPa min^{-1}. Finally, the system was flushed with nitrogen and allowed to cool to ambient temperature.

Low-temperature (LT) supercritical drying. Semicontinous extraction of the alcogels with supercritical carbon dioxide ($T_c = 304$ K, $p_c = 7.38$ MPa, (44)) was performed in an autoclave system using 100-ml additional ethanol and a turbine stirrer (60 rpm) to minimize temperature

TABLE 1

Chemical and Morphological Properties of Copper/Zirconia and Silver/Zirconia Aerogels Calcined at 573 K in Air

Aerogel	Sol-gel process	Acid	S_{BET} ($m^2 \cdot g^{-1}$)	$V_p(N_2)$[a] ($cm^3 \cdot g^{-1}$)	$\bar{d}_p$[b] (nm)	$d_{p,max}$[b] (nm)	$\bar{d}_{Metal}$(XRD)[c] (nm)	$S_{Cu}(N_2O)$[d] ($m^2 \cdot g^{-1}$)	Metal/Zr ratio[e] raw	Metal/Zr ratio[e] calcined
HT-Cu/ZrO_2	Two stage	HAc	128	0.27		4/74	33	0.8	0.005	0.04
HT-Cu/ZrO_2	One stage	HAc	100	0.21		3/64	31	—	0.010	0.11
HT-Cu/ZrO_2	One stage	HNO_3	143	0.81	23	23	28	1.3	0.007	0.07
LT-Cu/ZrO_2	One stage	HNO_3	139	0.74	20	24	—[f]	5.0	0.030	0.15
HT-Ag/ZrO_2	Two stage	HAc	99	0.24		4/76	5	-	0.090	0.10
HT-Ag/ZrO_2	One stage	HAc	77	0.14		4/80	6	-	0.080	0.08
HT-Ag/ZrO_2	One stage	HNO_3	125	0.79	23	22	10	-	0.030	0.12
LT-Ag/ZrO_2	One stage	HNO_3	112	0.76	25	26	7	-	0.030	0.08

[a] V_p designates the BJH cumulative desorption pore volume of pores in the range 1.7–300 nm.
[b] Mean pore diameter, $\bar{d}_p = 4\,V_p(N_2)/S_{BJHdes}$; maximum of pore size distribution $d_{p,max}$ derived from the desorption branch of the isotherm.
[c] Metal crystallite size of uncalcined (raw) aerogels calculated from the half-width of the corresponding (111) reflections.
[d] Copper surface area measured by N_2O-titration after catalytic testing.
[e] Atomic ratio of copper and silver, respectively, to zirconium calculated from the corresponding XPS data.
[f] Could not be resolved by XRD.

inhomogeneities. At a temperature of 313 K, the autoclave was pressurized with CO_2 to 24 MPa and the liquid–gas separator to 1 MPa, which resulted in an overall amount of 2.3 kg of CO_2. Subsequently, ethanol was semicontinously extracted for 5 h at 313 K using a CO_2 flow of 20 $g \cdot min^{-1}$. The pressure was then isothermally released with a mass flow of 20 $g \cdot min^{-1}$. After cooling to ambient temperature, the aerogel clumps were ground in a mortar.

Thermal treatment. To remove most of the organic residues prior to calcination, the raw aerogel samples were pretreated in flowing nitrogen (500 $ml \cdot min^{-1}$) by heating at 5 $K \cdot min^{-1}$ to 573 K with a dwell time of 1 h. After cooling to 353 K the samples were calcined in flowing air (500 $ml \cdot min^{-1}$) by heating at 5 $K \cdot min^{-1}$ to 573 K, followed by an isothermal step of 4.5 h at 573 K.

Physicochemical Characterization

The physicochemical properties of the catalysts were characterized by means of nitrogen physisorption, X-ray diffraction (XRD), transmission electron microscopy (TEM), X-ray photoelectron spectroscopy (XPS), thermal analysis (DTA/TG), temperature-programmed reduction (TPR), and nitrous oxide titration.

The specific surface areas (S_{BET}) and the mean pore diameters ($\bar{d}_p$) of the samples were determined by nitrogen physisorption at 77 K using a Micromeritics ASAP 2010 instrument. Prior to measurements, the samples were degassed for 5 h at 473 K. Pore size distributions were calculated applying the Barrett–Joyner–Halenda (BJH) method to the desorption branch of the isotherms. The assessment of microporosity was made from *t*-plot constructions ($0.3 < t < 0.5$ nm), using the Harkins–Jura correlation. For further details refer to Ref. (45).

X-ray powder diffraction patterns were measured on a Siemens θ/θ D5000 powder diffractometer in a step mode (step size 0.01° 2θ) using Ni filtered Cu Kα radiation. The patterns obtained were compared with JCPDS data files (JCPDS Mineral Powder Diffraction Data Files, Park Lane, PA). The mean crystallite sizes of Cu and Ag were calculated from the half-width of the corresponding (111) reflection, using the Scherrer equation and assuming spherical crystallites.

Samples for transition electron microscopy (TEM) were crushed and deposited on a holey carbon foil supported by a copper grid. The Philips CM30 microscope, operated at 300 kV, was equipped with Supertwin lens (cs = 1.2 mm, point resolution <0.2 nm).

X-ray photoelectron spectra were recorded with a Leybold-Heraeus LHS 11 instrument using MgKα (1253.6 eV) radiation and a stainless steel sample holder. The base pressure of the apparatus was lower than 5×10^{-10} mbar. The hemispherical analyzer was set to a constant pass energy of 38 eV at an energy scale calibrated versus the Au $4f_{7/2}$ signal at 84.0 eV. The energy resolution was 0.9 eV (Ag $3d_{5/2}$). Corrections of the energy shift due to steady state charging effects were accomplished by assuming the Zr $3d_{5/2}$ line of the ZrO_2 support as lying at 182.3 eV (46). Due to the overlap of the C 1s signals, deconvolution of the peaks was necessary. The fitting function used was a mixed Lorentzian/Gaussian function with a Lorentz/Gauss ratio of 0.8. The FWHM of the corresponding peaks was set to a constant value of 2.4 eV. Constant binding energy values were used for the contributions due to C–H (285.0 eV) (47), C–O (286.4 eV) (48), and C=O (289.2 eV) (49). Quantification of the spectra was done by integration of the peaks (Cu $2p_{3/2}$, Ag 3d, O 1s, C 1s, Zr 3d) after subtraction of a Shirley-type background (50) using empirically derived cross section factors (51).

The apparatus used for the TPR studies has been described in detail previously (52). TPR profiles were measured under the following conditions: heating rate 10 $K \cdot min^{-1}$, flow rate 75 $cm^3 \cdot min^{-1}$ 5% H_2/Ar.

Copper surface areas were determined by nitrous oxide titration using a pulse technique similar to that reported by Evans *et al.* (53). Samples were first reduced in flowing H_2/Ar (5% H_2, 75 $cm^3 \cdot min^{-1}$) by heating at 5 $K \cdot min^{-1}$ from 373 to 493 K. Subsequently the samples were held at this temperature for 30 min and then exposed to a flux of 75 $cm^3 \cdot min^{-1}$ of pure hydrogen for 30 min at the same temperature. The hydrogen was purged with 50 $cm^3 \cdot min^{-1}$ He at 493 K. After cooling to 363 K under He, pulses of nitrous oxide (0.5 cm^3) were injected. Copper metal surface areas were calculated assuming 1.46×10^{19} copper atoms per m^2 (53) and an adsorption stoichiometry of $Cu_s/O_{ads} = 2$. Back titration of the oxidized copper surface was carried out using pulses of CO (0.5 cm^3) at 423 K.

Catalytic Tests

The apparatus used for the catalytic tests consisted of a continuous tubular flow fixed-bed microreactor which was operated at 1.7 MPa total pressure. Feed and product gas analysis was performed using a Hewlett Packard model 5890A gas chromatograph equipped with a thermal conductivity detector. Product separation was achieved with a stainless steel column (5 m, 1/8 inch OD) containing 80–100 mesh Porapak QS.

Standard experiments in the temperature range 453 to 533 K were carried out using 1.0 g of catalyst (1.3 g in case of raw LT-aerogels) under a reactant flow rate of 90 $cm^3 \cdot min^{-1}$ (STP) CO_2/H_2 (1/3). The reactant gas mixture, containing CO_2 (99.9%) and H_2 (99.999%), was fed from a high pressure cylinder without further purification, using a Brooks mass flow controller. The prereduction of the catalysts (50–150-μm sieve fraction) was performed in the apparatus used for activity measurements, according to the following procedure: heating to 473 K at a heating rate of 15 $K \cdot min^{-1}$ in 1.25 vol% H_2/N_2 at a pressure of 10^5 Pa. The H_2-concentration was then increased stepwise (30 min

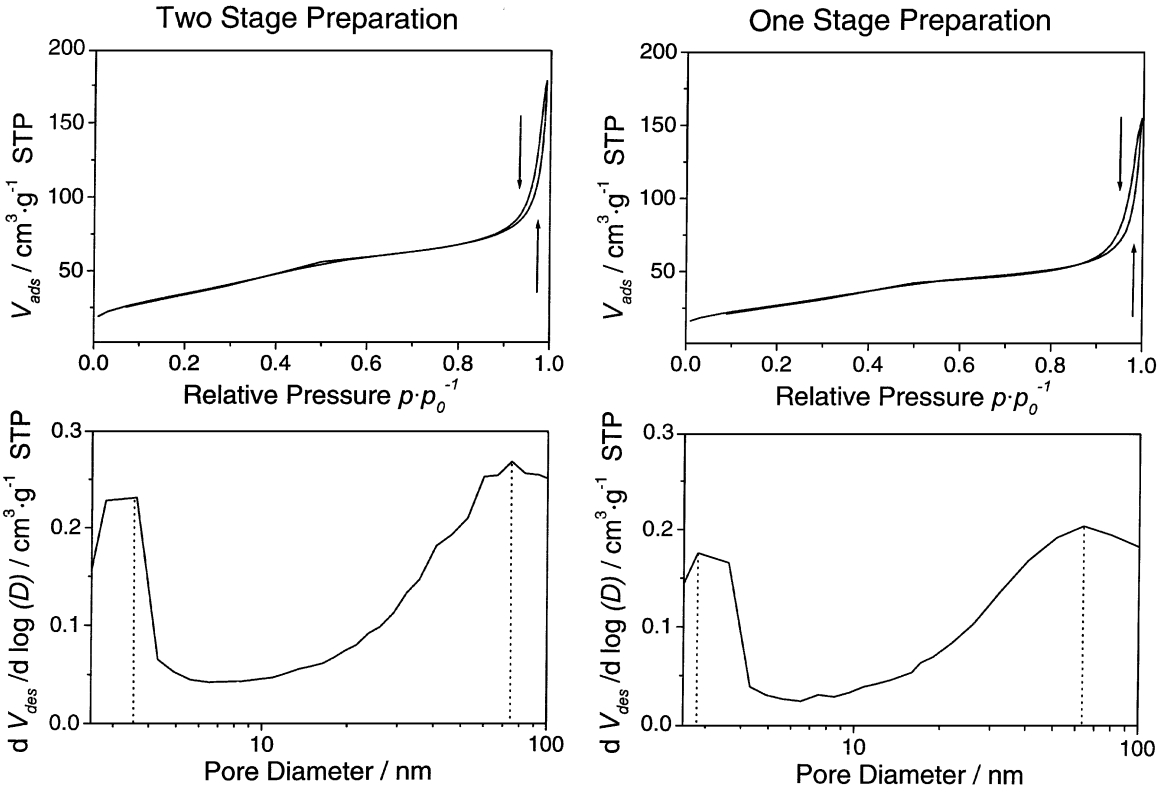

FIG. 1. Influence of wet-chemical preparation procedure on isotherms and pore-size distributions of HT-copper zirconia aerogels prepared using acetic acid. Both samples were calcined in air at 573 K. Top: adsorption(↑)/desorption(↓) isotherms; bottom: pore-size distribution derived from the desorption branch.

per step) in the sequence 2.5/5/10/20/50 to 100%. After replacement of H_2 with reactant gas the temperature was brought to 533 K under a pressure of 1.7 MPa and kept at this temperature for 4 h.

Activities and selectivities were determined at steady state after the catalyst had been on stream for 15 h at 493 K. Conversions, typically in the range 0.5–10%, are defined as: (moles carbon dioxide converted to all products)/(initial concentration of carbon dioxide). The selectivity is defined as: (moles carbon dioxide converted to product *i*)/(moles carbon dioxide converted to all products).

RESULTS

The structural and chemical properties of the Cu/ZrO_2 and Ag/ZrO_2 aerogels with 10 at% metal loading are summarized in Table 1.

Nitrogen Physisorption

After calcination in air at 573 K all aerogels showed a type-IV isotherm with a type-H3 desorption hysteresis according to IUPAC classification (54), which is characteristic of well-developed meso- to macroporous materials. Typical adsorption/desorption isotherms and pore-size distributions of the copper–zirconia HT-aerogels prepared with acetic acid, using the one-stage and two-stage preparation procedure, are compared in Fig. 1. In addition to the major hysteresis loop above $p \cdot p_0^{-1} = 0.9$, both samples show some indication of a minor hysteresis loop around a relative pressure of $p \cdot p_0^{-1} = 0.5$. Independent of the preparation procedure, all aerogels prepared with acetic acid revealed a bimodal pore-size distribution with maxima around 3 nm, indicating small mesopores, and around 70 nm, characteristic for macropores (Table 1). In addition, *t*-plot analysis revealed a small contribution of micropores for these catalysts.

The adsorption/desorption isotherms and pore-size distributions of the differently dried silver–zirconia aerogels, prepared with nitric acid and calcined at 573 K in air, are depicted in Fig. 2. Independent of the drying procedure, the samples show a type-IV isotherm with type-H3 hysteresis and a similar unimodal pore-size distribution with maxima in the range 22–26 nm. In contrast to the aerogels prepared with acetic acid no indication of micropores is discernible from calculated *t*-plots.

A comparison between the differently prepared samples calcined in air at 573 K revealed generally lower surface areas, specific pore volumes and average pore-size diameters for samples prepared with acetic acid (Table 1). Independent of the drying procedure, highest surface areas

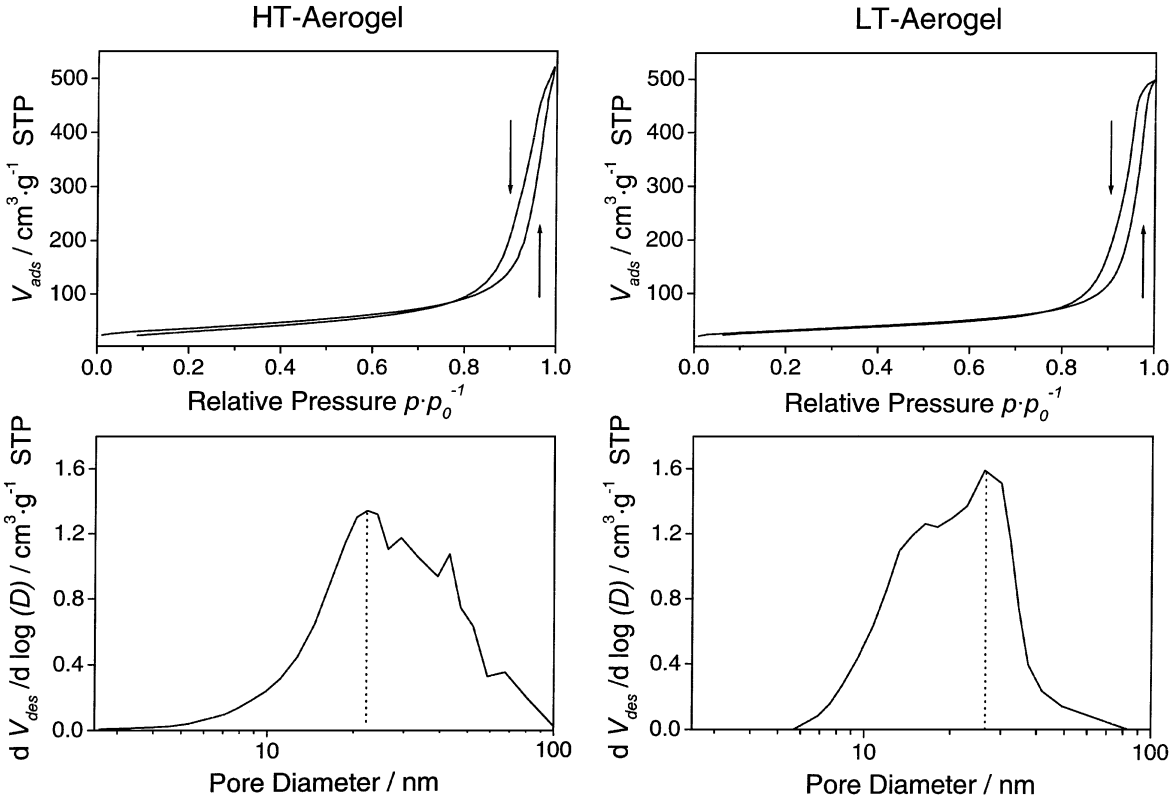

FIG. 2. Influence of drying method on isotherms and on pore-size distributions of silver zirconia aerogels prepared using nitric acid. Both samples were calcined in air at 573 K. Top: adsorption(↑)/desorption(↓) isotherms; bottom: pore-size distribution derived from the desorption branch.

(112–143 $m^2 \cdot g^{-1}$) and specific pore volumes (0.74–0.81 $cm^3 \cdot g^{-1}$) were observed for samples prepared with nitric acid, but with the high temperature supercritically dried aerogels showing slightly higher values. As concerns the influence of the metal component, it follows from Table 1 that the silver-containing samples show lower S_{BET}, but similar porosity. Two-stage preparation resulted in higher surface areas and specific pore volumes compared to one-stage preparation.

X-ray Diffraction and Transition Electron Microscopy

The influence of acid used in the sol-gel process, drying method, and calcination on the phase composition of the aerogels is shown in Figs. 3 and 4 for copper–zirconia and silver–zirconia, respectively. The XRD patterns of the raw aerogels are almost independent of the metal component and of the acid used. In agreement with previous observations on pure zirconia aerogels (43, 45, 55), the crystalline fraction of all HT-aerogels consisted of predominantly tetragonal ZrO_2 with a minor contribution of monoclinic zirconia. As regards the metal component, characteristic reflections due to metallic copper and silver, respectively, are observed for the raw samples. The mean size of the copper crystallites (Table 1), estimated from the line broadening of the corresponding (111) reflection, was similar for all

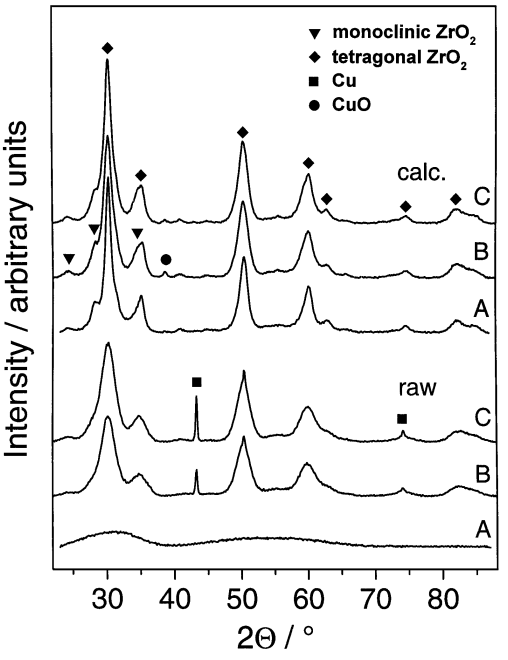

FIG. 3. XRD patterns of copper zirconia aerogels, raw (bottom series), and calcined in air at 573 K (top series). Effect of acid and drying method on phase composition. (A) LT-aerogel prepared using nitric acid, (B) HT-aerogel prepared using nitric acid, and (C) HT-aerogel prepared using acetic acid (one stage preparation).

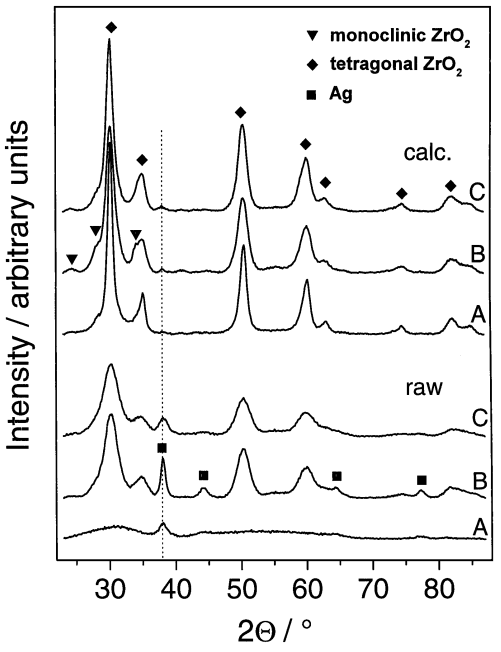

FIG. 4. XRD patterns of silver zirconia aerogels, raw (bottom series) or calcined in air at 573 K (top series). Effect of acid and drying method on phase composition. (A) LT-aerogel prepared using acetic acid, (B) HT-aerogel prepared using nitric acid, and (C) HT-aerogel prepared using acetic acid (one stage).

HT-aerogels (ca 30 nm). In contrast, the mean size of the silver crystallites was slightly higher for the sample prepared with nitric acid (10 nm) as compared to the HT-aerogels prepared with acetic acid (5–7 nm). Calcination at 573 K in air resulted in the oxidation of copper to mainly X-ray amorphous copper oxide and in a slight increase of the monoclinic zirconia shares in all HT-aerogels, particularly for the aerogels prepared with nitric acid. In contrast, the calcined silver-containing aerogels showed only traces of silver and no silver oxide was detectable (Fig. 4).

XRD patterns of the raw LT-aerogels indicated the presence of X-ray amorphous zirconia besides weak reflections due to crystalline silver (Fig. 4), whereas no reflections due to crystalline copper species were discernible (Fig. 3). Calcination at 573 K transformed both samples to mainly tetragonal ZrO_2, which exhibits a clearly larger crystallite size (7–9 nm), compared to the corresponding HT-aerogels (5 nm). Reflections characteristic for Cu or CuO, and Ag or Ag_2O were not observed with the calcined LT-aerogels.

In agreement with X-ray line-broadening measurements a mean size of the zirconia crystallites around 5 nm is observed for the calcined HT silver–zirconia aerogel prepared with nitric acid (Fig. 5). TEM showed primary particles, which remain the same for all samples.

XPS Analysis

XPS analysis was performed to study the influence of the preparation variables on the nature and the relative concentration of the surface species. Measurements were carried out with raw aerogels and with samples calcined in air at 573 K. XP-spectra of the C 1s region are shown in Fig. 6 for the raw HT and LT copper–zirconia aerogel, respectively, prepared with nitric acid. For analysis the XP spectra were deconvoluted into three peaks with binding energies characteristic for C−H (47), C−O (48), and C=O (49). The signal at ca 283 eV originated from carbon fragments on the uncharged sample holder. Clearly, the sample dried at low temperatures contained a higher ratio of oxygen containing carbon species, whereas on the HT-aerogel predominantly C−H type species were present.

The semiquantitative analysis of the XP-spectra revealed a high proportion (19–23 at%) of carbon on the surface of the raw aerogels, which decreased substantially to 5.7–7.4 at% upon calcination in air at 573 K. No significant effect of the drying procedure on the carbon content was evident. Except for the silver–zirconia aerogels prepared with acetic acid, the metal/zirconium ratio on the surface of the raw aerogels was significantly lower (0.005–0.03) than expected from the bulk composition of the samples (Table 1). Calcination at 573 K resulted in an increase of the surface concentration of the metal, affording metal/zirconium ratios, which roughly resemble the bulk composition of the samples. As can be seen from Table 1, the effect of calcination is more pronounced for the copper-containing samples. As concerns the change in metal/zirconia ratio (XPS) there are two factors which have to be considered, (i) oxidation/redispersion of the metal particles and (ii) oxidation of carbonaceous residues. Based on the data listed in Table 1 we suggest that segregation/redispersion is the dominating factor.

Thermal Analysis

A high content of organic residues in the raw aerogels was also evidenced by the thermal analysis performed in flowing air. Representative for all samples, which showed a comparable behavior, the thermoanalytical results for the raw LT silver–zirconia aerogel prepared with nitric acid are presented in Fig. 7. The observed weight loss originated from the evolution of water (desorption of physisorbed water, dehydroxylation) and from the oxidation of organic residues. This emerges from relating the TG curve to the monitored ion intensities of $m/z = 44$ (CO_2^+) and $m/z = 18$ (H_2O^+). The evolution of water began at ambient temperature and reached maxima at ca 420 and 563 K. The first H_2O evolution originated mainly from physisorbed water, combined with a minor contribution from the oxidation of organic species adsorbed on the aerogel surface, as evidenced by the weak CO_2 peak at the same temperature. At higher temperatures the liberation of adsorbed water was superseded by the contribution of H_2O originating from the oxidation of organic residues (strong peak at 563 K). Pronounced CO_2 evolution started at ca 500 K and attained its

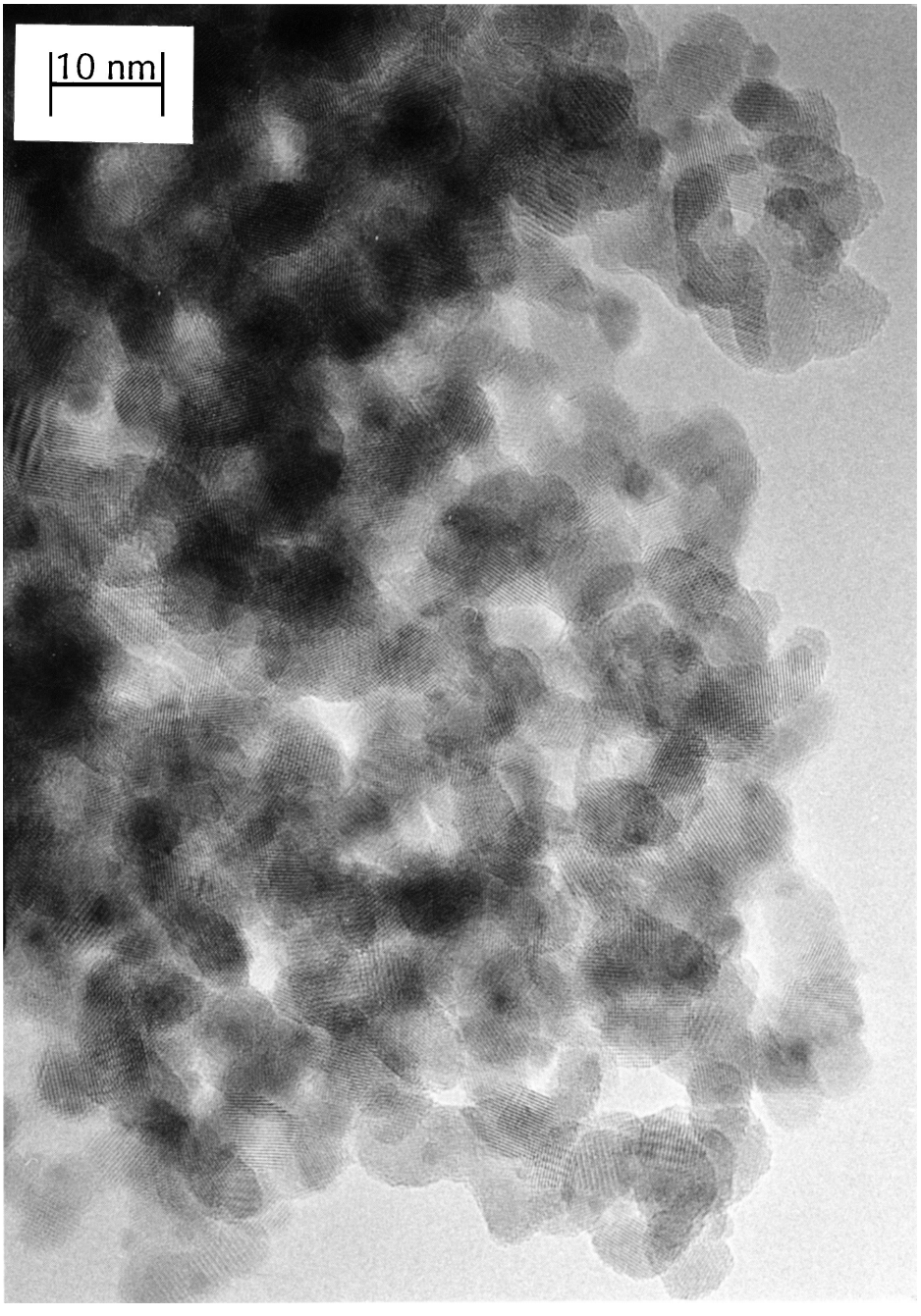

FIG. 5. High-resolution transmission electron micrograph of the HT silver-zirconia aerogel prepared with nitric acid and calcined at 573 K, after catalytic testing, showing typical structure of zirconia as present in all samples.

maximum at 563 K. The oxidation of organic residues is also evidenced by the exothermic peaks at 423 and 576 K in the DTA curve. A weak signal at 773 K can be attributed to the crystallization of amorphous zirconia in the LT-aerogels. For the copper containing LT-aerogel crystallization took place at 830 K.

In case of the high temperature dried aerogels no indication for the oxidation of organic species adsorbed on the aerogel surface (peak at ca 410 K) was observed. Moreover, significantly less water evolved from these samples up to 500 K. This is also indicated by the overall weight loss of the samples in the thermoanalytical experiments, which amounted to 11–13% for the HT-aerogels and to 26–30% for the LT-aerogels for a temperature of 700 K.

TPR Measurements. The reduction characteristics of the differently dried copper–zirconia aerogels are depicted in Fig. 8. TPR profiles of the samples calcined in air at

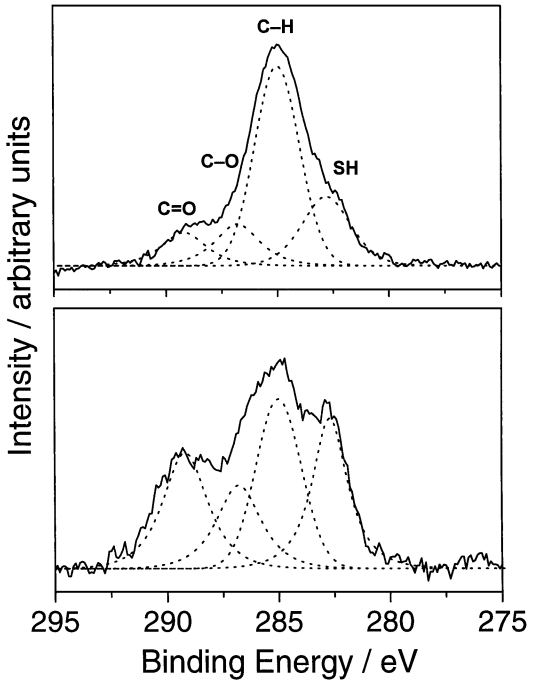

FIG. 6. XP-spectra of the C 1s region of the raw LT-Cu/ZrO_2 aerogel (bottom) and of the raw HT-Cu/ZrO_2 aerogel prepared using nitric acid (top). Details of deconvolution are given in the Experimental section. SH indicates carbon fragments on the sample holder.

573 K exhibit two reduction peaks in the range 447–521 K, characteristic for the reduction of copper oxide. The occurrence of two reduction peaks indicates the presence of copper oxide species differently interacting with the zirconia matrix. Note that in case of the HT-aerogel higher temperatures are required for complete reduction of CuO. In contrast to the calcined samples reduction of the raw LT copper–zirconia aerogel occurred at significantly higher temperatures. The negative peak observed at 774 K can either be assigned to the desorption of hydrogen from the catalyst surface or, more probably, to the decomposition of hydrocarbon residues in the catalyst originating from the sol-gel process.

In case of the raw silver–zirconia LT-aerogel, a single peak at 526 K was observed in the TPR profile (Fig. 9), indicating the reduction of oxidized silver species. The negative peak observed at 750 K can be again assigned to the decomposition of hydrocarbon residues in the catalyst originating from the sol-gel process. This is supported by the TPR profile of the sample calcined at 573 K in air, which showed no negative peak. Calcination, moreover, resulted in a shift of the peak due to the reduction of silver oxide to 352 K. The weak broad peak in the TPR profile at 753 K can be caused by reduction of silver oxide species strongly interacting with the zirconia matrix or by partial reduction of the zirconia surface. Quantification of the hydrogen consumed in the TPR indicated that only part of the silver was present as silver oxide (Ag_2O) at the beginning of the measurement.

Catalytic Behavior in CO_2 Hydrogenation

The catalytic performance of the aerogels was investigated after drying as well as after calcination in air at 573 K. The only carbon-containing products found were methanol and carbon monoxide, except for the calcined silver–zirconia aerogels (LT, HT) prepared with nitric acid, which produced traces of methane at 533 K.

Figure 10 illustrates the effects of preparation conditions, calcination, and drying method on the temperature dependence of CO_2-consumption and methanol selectivity for the copper–zirconia aerogels. As indicated by Fig. 10A (bottom), the use of either acetic or nitric acid in the sol-gel process did not significantly influence the catalytic behavior of the calcined copper catalysts prepared by high temperature supercritical drying. In contrast, the influence of calcination was significant for the initially X-ray amorphous LT-aerogel, as indicated by the CO_2-consumption and selectivity behavior shown in Fig. 10B (middle). CO_2-consumption was clearly higher for the calcined aerogel, but with increasing temperature selectivity to methanol decreased more pronounced for this sample, compared to the raw aerogel. Catalytic data for the low- and high-temperature supercritically dried and calcined aerogels are presented

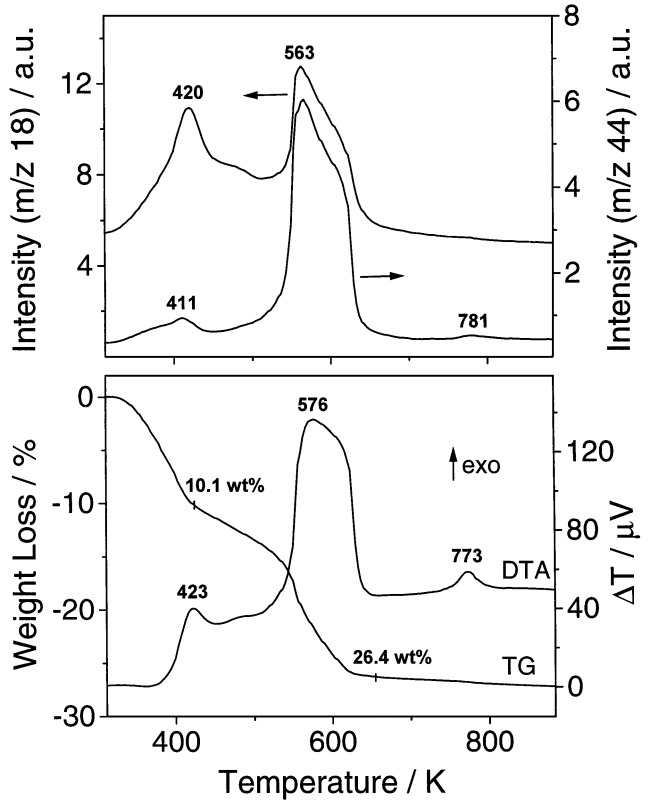

FIG. 7. Combined TG/DTA and MS-investigation of raw Ag/ZrO_2 LT-aerogel prepared with nitric acid. Top: ion intensities of m/z = 18 (H_2O^+) and m/z = 44 (CO_2^+); bottom: TG and DTA curves. Heating rate, 10 K · min^{-1}; air flow, 25 cm^3 · min^{-1}.

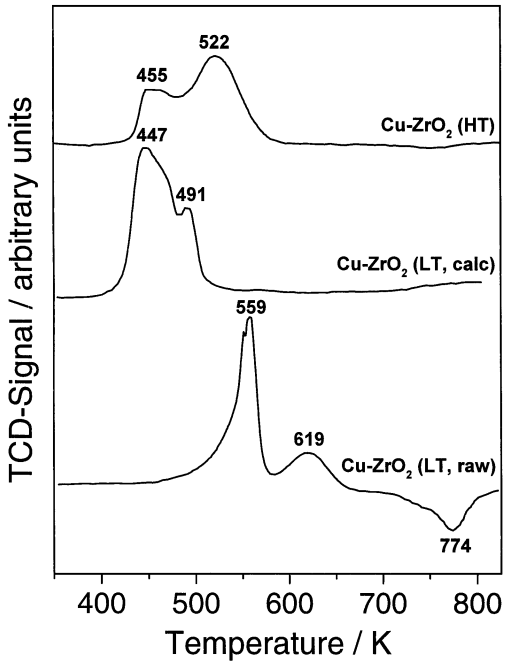

FIG. 8. Temperature-programmed reduction profiles of the raw and calcined copper–zirconia LT-aerogels and of the calcined copper–zirconia HT-aerogel prepared with acetic acid (two stage). TPR in 5% H_2/Ar, 10 K · min^{-1}.

in Fig. 10C (top), together with corresponding data for a xerogel calcined in air at 623 K (S_{BET} = 213 m^2 · g^{-1}; V_p = 0.13 cm^3 · g^{-1}; data taken from Ref. (25)). Whereas the temperature dependency of methanol-selectivity was similar

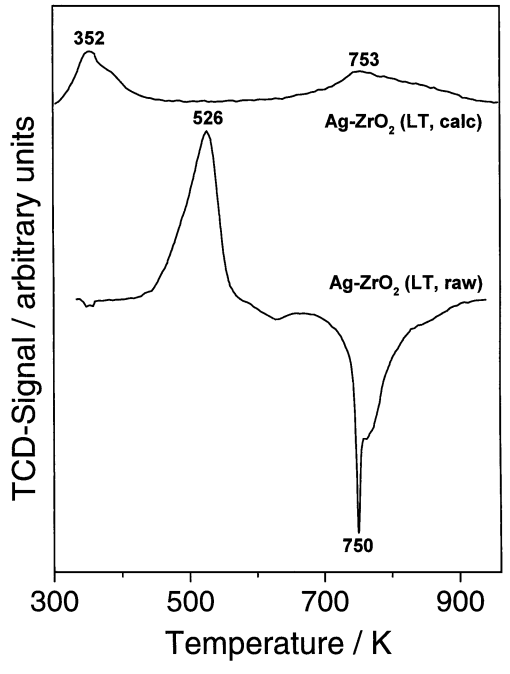

FIG. 9. Temperature-programmed reduction profiles for the raw and calcined silver–zirconia LT-aerogels. TPR in 5% H_2/Ar, 10 K · min^{-1}.

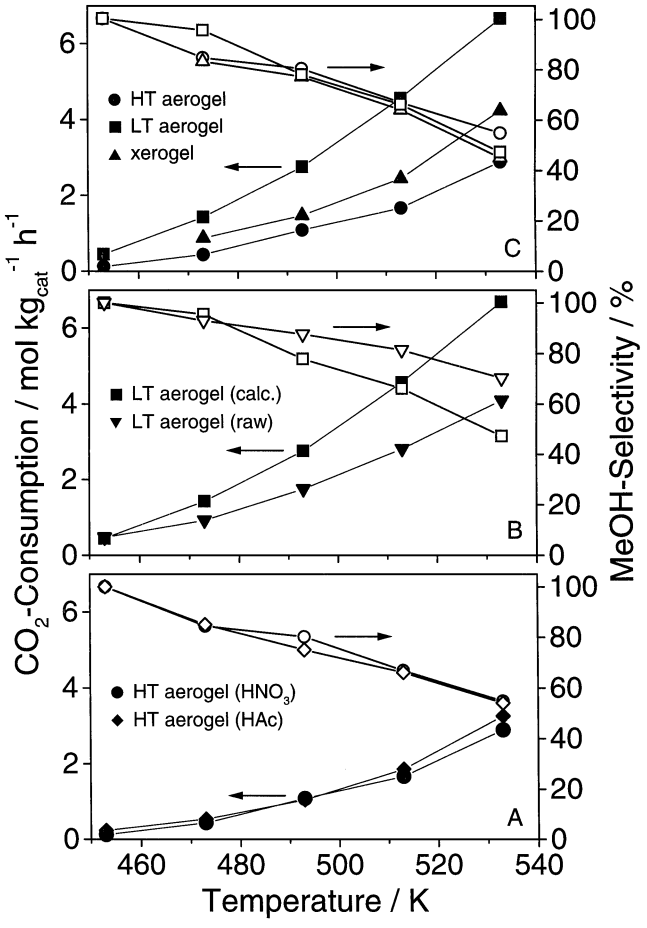

FIG. 10. Catalytic results of carbon dioxide hydrogenation over copper-zirconia. Effect of (A) preparation conditions, (B) calcination, and (C) drying method on CO_2-consumption rate and selectivity to methanol. Data for the xerogel are taken from (12). Conditions: 1-g catalyst (1.3 g for dried sample), 90 cm^3 · min^{-1}, H_2/CO_2 = 3, 1.7 MPa.

for all catalysts, CO_2-consumption decreased in the order LT-aerogel > xerogel > HT-aerogel.

Catalytic data for the calcined silver–zirconia catalysts are depicted in Fig. 11. Similar to copper–zirconia, the drying method had no significant influence on the methanol selectivity. Moreover, no difference in CO_2-consumption was discernible for the LT- and HT-aerogels, which contrasts the findings for copper–zirconia, where CO_2-consumption was substantially higher for the LT-aerogel. Catalytic behavior comparable to that with aerogels was observed for the xerogel at lower temperatures, whereas at higher temperatures an increase in CO_2-consumption was less pronounced for the xerogel calcined at 623 K (S_{BET} = 170 m^2 · g^{-1}; V_p = 0.21 cm^3 · g^{-1}; data taken from Ref. (25)). As regards the catalytic behavior of the raw LT-aerogel Ag/ZrO_2, no methanol formation and only a small amount of CO (0.35 mol%) were found at 533 K. At higher temperatures, where sintering of silver starts to occur, traces of methanol and increasing CO-production were observed.

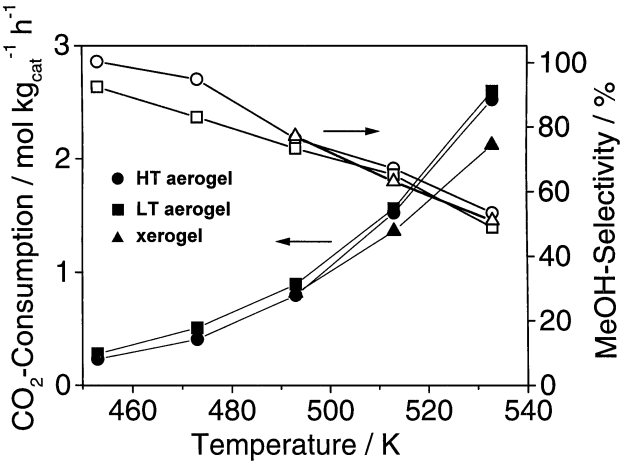

FIG. 11. Influence of the drying method on CO_2-consumption rate and selectivity to methanol in carbon dioxide hydrogenation over calcined silver–zirconia catalysts prepared with HNO_3. Data for the xerogel are taken from (12). Conditions: 1-g catalyst, 90 $cm^3 \cdot min^{-1}$, $H_2/CO_2 = 3$, 1.7 MPa.

Finally, comparing the catalytic behavior of the IB metal-zirconia LT-aerogels, Fig. 12 reveals a markedly higher activity for copper–zirconia, whereas selectivity to methanol is similar for both catalysts.

DISCUSSION

Structural Properties of Aerogels

Independent of the drying conditions, the aerogels calcined at 573 K possess similar BET surface areas, with the silver-containing samples showing consistently lower values. Generally, the use of acetic acid in place of nitric acid, as well as application of a two-step (ts) preparation procedure, results in lower S_{BET} (Table 1). The results of nitrogen physisorption confirm earlier findings about the influence of the acid used in the sol-gel process on the pore-size distribution of the aerogels (43, 45), showing substantially lower specific pore volumes and a bimodal pore-size distribution with a contribution of micropores for samples prepared with acetic acid. Comparison of the BET surface area of pure zirconia aerogels (43, 55) with aerogels containing IB metals reveals a marked decrease of S_{BET} for the HT-aerogels containing silver or copper, whereas no significant effect is observed for the LT-aerogels. The significantly higher pore volume of the LT-aerogels compared to the HT-aerogels can be traced back to the high content of organic residues in the LT-aerogels, which evolve as gases (CO_2, H_2O) during calcination, thus expanding the material and leading to a large-pore volume.

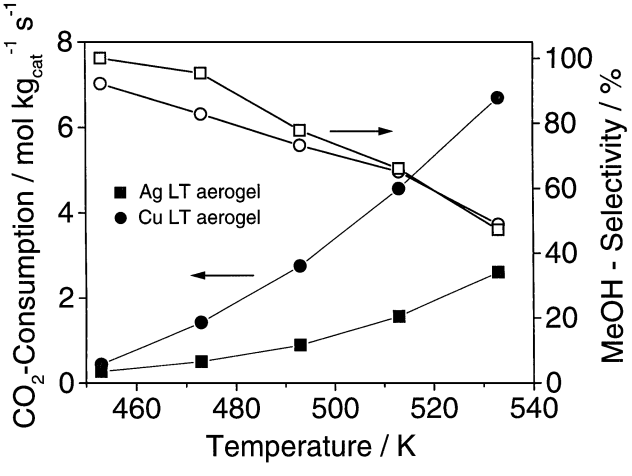

FIG. 12. Comparison of catalytic behavior of calcined copper–zirconia and silver–zirconia LT- aerogels in carbon dioxide hydrogenation. Conditions: 1-g catalyst, 90 $cm^3 \cdot min^{-1}$, $H_2/CO_2 = 3$, 1.7 MPa.

XRD-measurements reveal the presence of X-ray amorphous zirconia for raw LT-aerogels, whereas crystalline ZrO_2 is present in the raw HT-aerogels. The appearance of crystalline ZrO_2 in the HT-aerogels contrasts the findings of Sun and Sermon (40–42), who observed X-ray amorphous zirconia for similarly dried samples, which were, however, prepared from copper– and zirconyl–nitrate by gel-precipitation with KOH at pH 10 in an aqueous media. In this case, contaminants originating from the precursor materials used, e.g. potassium residues, can stabilize zirconia in its amorphous state (22). Benedetti *et al*. (56, 57) recently demonstrated the importance of sodium ions for stabilizing zirconia. The presence of metallic silver and copper in samples dried at high temperatures can be explained by the reduction potential of ethanol under the supercritical drying conditions applied. Comparison of the average metal crystallite size shows substantially larger particles for copper, which may be due to increased sintering effects occurring with copper during supercritical drying. Another reason could be that in the case of copper–zirconia particle formation and reduction of copper ions occurred mainly during supercritical drying, whereas the silver acetate containing solution turned from milky-white into black within minutes during sol-gel processing, indicating that formation of metal oxide or metal particles took place already during the wet-chemical preparation procedure. This assumption is supported by the occurrence of metallic silver also in the LT-aerogel and by analogous observations for platinum- and palladium-titania aerogels, respectively, dried at high temperatures (34, 35). In contrast, no evidence for the presence of crystalline copper species is found in the XRD pattern of the LT copper–zirconia aerogel. TPR indicated that this sample predominantly contained copper oxide species.

As concerns the influence of the preparation conditions (type of acid, one-step or two-step procedure, type of supercritical drying) on the metal dispersion, they all have little effect with Cu/ZrO_2. Regardless of the conditions applied the mean copper crystallite size varies only in the range

28–33 nm. In contrast the mean silver crystallite size increased significantly when HNO_3 was employed instead of HAc (Table 1). The reason for this behavior is not clear yet.

DTA measurements show a stabilization of the amorphous zirconia phase in the presence of copper or silver, as reported earlier (20, 22, 24). This is evidenced by the temperature of crystallization of the X-ray amorphous zirconia, which is higher for Cu/ZrO_2 (830 K) compared to Ag/ZrO_2 (770 K), and clearly higher than for pure ZrO_2 (715 K, (58)). As previously observed (55, 58), zirconia crystallites are larger for the calcined LT-aerogels compared to the calcined HT-aerogels, which are already crystalline after drying. Taking into account data of the DTA experiments, crystallization of the initially X-ray amorphous zirconia in the LT-aerogels upon calcination at 573 K was not expected. If calcination was carried out with a very low amount of sample, the aerogels remained X-ray amorphous, indicating that the high content of organic residues in the raw aerogels probably results in hot spots and thus facilitates crystallization. Calcination, moreover, transformed metallic copper of the HT-aerogels to X-ray amorphous copper oxide, thus indicating a high dispersion of the copper species. In case of silver–zirconia, weak reflections due to metallic silver remain in the XRD spectra after calcination. TPR measurements show a shift of the reduction peak for silver oxide to lower temperature and a significantly lower hydrogen consumption for the calcined LT-aerogel, indicating that silver was predominantly redispersed as silver metal and not oxidized to Ag_2O.

Catalytic Behavior in CO_2-Hydrogenation

Copper- and silver–zirconia aerogels are active and selective catalysts for the synthesis of methanol, but with Cu/ZrO_2 being substantially more active, as has been shown previously for coprecipitated catalysts (24, 25). Besides of methanol formation, both catalysts facilitate the water–gas shift reaction, thus producing carbon monoxide as a by-product.

In contrast to Cu/ZrO_2, no activity for methanol formation is observed for the uncalcined Ag/ZrO_2 LT-aerogel. Calcination of the raw LT-aerogels in air at 573 K causes a marked increase of activity for both IB metals. Note that the raw aerogels contain large amounts of organic residues, which presumably block active sites and which are removed upon calcination. Compared to methanol synthesis, activity for the reverse water–gas shift reaction increased stronger upon calcination, resulting in lower methanol selectivity. The calcined copper–zirconia aerogels produced by low-temperature supercritical drying was markedly more active and similarly selective for methanol synthesis than the sample prepared analogously, but dried at high temperatures. In case of silver-zirconia no such difference can be observed. Both the LT- and HT-aerogels possess comparable textural properties (Table 1). However, N_2O-titration and XPS measurements reveal a clearly higher copper surface area for the Cu/ZrO_2 LT-aerogel, whereas in the case of the silver aerogels XRD indicates similar silver crystallite sizes for the high- and low-temperature dried samples (Table 1). The latter is supported by the comparable silver/zirconia ratio observed with XPS. As regards the zirconia phase, crystallite sizes remained almost unchanged upon catalytic testing and are larger for the LT-aerogels compared to the HT-aerogels. The present results indicate that for the similarly prepared aerogel catalysts the activity is related to the number of copper centers exposed. The assumption that the copper surface area is solely responsible for catalytic activity has been disputed in the literature (18, 22, 59, 60) and it has been proposed that catalytic performance in methanol synthesis is strongly dependent on the interfacial metal–oxide contact area (20, 22, 25, 60).

As concerns methanol synthesis the activity of silver, which is usually regarded as inactive, Frost reported substantial activity for silver supported on thoria (60). This contrasts the findings of Shaw *et al.* (61) who observed no significant activity for catalysts derived from intermetallic silver, copper, and cerium alloys. Nonneman and Ponec (62) suggested that the different results concerning the activity of silver catalysts for methanol synthesis may be related to contaminants originating from the precursor materials used. In previous studies on Ag/ZrO_2 xerogel catalysts prepared by precipitation of metal nitrates with NaOH, an influence of contaminants on methanol synthesis activity could not be completely ruled out (24, 25). In the present work, which uses silver–zirconia aerogel catalysts prepared by a solution sol-gel procedure with pure alkoxide precursors, contamination by alkaline components can be excluded, thus indicating that activity is directly related to the silver–zirconia system.

Comparing the catalytic data for the copper–zirconia aerogel catalysts with previously reported results obtained with xerogel-type catalysts prepared by coprecipitation (25) shows superior activity in methanol synthesis for the LT-aerogel, whereas the HT-aerogel is less active. Methanol selectivity is similar for all samples. The superior performance of the LT-aerogel can be explained by its favorable textural properties, combined with a high copper surface area. A high portion of micropores and a lower copper surface area is found for the xerogel which, on the other hand, contained amorphous zirconia. In the case of silver–zirconia methanol production of both aerogels is slightly higher for temperatures exceeding 500 K, compared to the xerogel.

CONCLUSIONS

The performance of differently prepared copper–zirconia and silver–zirconia aerogels in the synthesis of

methanol from carbon dioxide and hydrogen has been examined. The influence of the wet chemical preparation conditions, of the supercritical drying procedure, and of calcination on the structural properties and on the catalytic behavior was investigated.

Extraction of the alcogels with supercritical carbon dioxide resulted in amorphous zirconia, whereas high-temperature supercritical drying afforded mainly tetragonal ZrO_2. The highly reducing conditions during high temperature drying led to the formation of copper crystallites with a mean size of 30 nm. In contrast, X-ray amorphous copper oxide existed in the LT-aerogels. N_2O titration revealed the highest copper surface for this catalyst, which was also most active in CO_2 hydrogenation. In the case of HT-aerogels the copper surface was much lower, leading to lower catalytic activity. For silver-containing samples, reduction occurred already during sol-gel processing, resulting in comparable silver crystallite sizes for raw aerogels, independent of the drying conditions. Similar activity in methanol synthesis was found for the different silver aerogels. With these catalysts, prepared by a solution sol-gel procedure using alkoxide and acetate precursors, contamination by alkaline components can be ruled out, indicating that activity is directly related to the silver–zirconia system.

ACKNOWLEDGMENTS

The authors thank Dr. M. Maciejewski for performing thermal analysis and Dr. U. Göbel for XPS measurements. Financial support of this work by the Bundesamt für Energiewirtschaft (Project-Nr. 21180) is gratefully acknowledged.

REFERENCES

1. Behr, A., *in* "Catalysis in C_1 Chemistry" (W. Keim, Ed.), p. 169. Reidel, Dordrecht, 1983.
2. Behr, A., *Angew. Chem., Int. Ed. Engl.* **27**, 661 (1988).
3. Chinchen, G. C., Denny, P. J., Jennings, J. R., Spencer, M. S., and Waugh, K. C., *Appl. Catal.* **36**, 1 (1988).
4. Halmann, M., "Chemical Fixation of Carbon Dioxide: Methods for Recycling CO_2 into Useful Products," CRC Press, Boca Raton, FL, 1993.
5. Baiker, A., and Koeppel, R. A., *in* "Proceedings, International Conference on Carbon Dioxide Utilization, Bari, Italy, 1993," p. 295.
6. Jessop, P. G., Ikariya, T., and Noyori, R., *Chem. Rev.* **95**, 259 (1995).
7. Baiker, A., and Koeppel, R. A., *in* "Proc., 3rd Int. Conf. on Carbon Dioxide Utilization, Norman, OK, 1995."
8. Leitner, W., *Angew. Chem, Int. Ed. Engl.* **34**, 2207 (1995).
9. Denise, B., and Sneeden, R. P. A., *Chemtech*, 108 (1982).
10. Mercera, P. D. L., Van Ommen, J. G., Doesburg, E. B. M., Burggraaf, A. J., and Ross, J. R. H., *Appl. Catal.* **57**, 127 (1990).
11. Ward, D. A., and Ko, E. I., *Chem. Mater.* **5**, 956 (1993).
12. Yamaguchi, T., *Catal. Today* **20**, 199 (1994).
13. Denise, B., and Sneeden, R. P. A., *Appl. Catal.* **28**, 235 (1986).
14. Denise, B., Sneeden, R. P. A., Beguin, B., and Chefiri, O., *Appl. Catal.* **30**, 353 (1987).
15. Amenomiya, Y., *Appl. Catal.* **30**, 57 (1987).
16. Amenomiya, Y., Emesh, A. I. T., Oliver, K. W., and Pleizier, G., *in* "Proc. 9th Int. Congr. Catal." (M. J. Phillips and M. Ternan, Eds.), p. 634. Chem. Inst. of Canada, Calgary, 1988.
17. Pommier, B., and Teichner, S. J., *in* "Proc. 9th Int. Cong. Catal." (M. J. Phillips and M. Ternan, Eds.), p. 610. Chem. Inst. of Canada, Calgary, 1988.
18. Denise, B., Cherifi, O., Bettahar, M. M., and Sneeden, R. P. A., *Appl. Catal.* **48**, 365 (1989).
19. Gasser, D., and Baiker, A., *Appl. Catal.* **48**, 279 (1989).
20. Köppel, R. A., Baiker, A., Schild, C., and Wokaun, A., *Stud. Surf. Sci. Catal.* **63**, 59 (1991).
21. Kanoun, N., Astier, M. P., and Pajonk, G. M., *Catal. Lett.* **15**, 231 (1992).
22. Köppel, R. A., Baiker, A., and Wokaun, *Appl. Catal.* **84**, 77 (1992).
23. Coteron, A., and Hayhurst, A. N., *Appl. Catal.* **101**, 151 (1993).
24. Fröhlich, C., Köppel, R. A., Baiker, A., Kilo, M., and Wokaun, A., *Appl. Catal. A* **106**, 275 (1993).
25. Baiker, A., Kilo, M., Maciejewski, M., Menzi, S., and Wokaun, A., *Stud. Surf. Sci. Catal.* **75**, 1257 (1993).
26. Nitta, Y., Fujimatsu, T., Okamoto, Y., and Imanaka, T., *Catal. Lett.* **17**, 157 (1993).
27. Nitta, Y., Suwata, O., Ikeda, Y., Okamoto, Y., and Imanaka, T., *Catal. Lett.* **26**, 345 (1994).
28. Fujitani, T., Saito, M., Kanai, Y., Kakumoto, T., Watanabe, T., Nakamura, J., and Uchijima, T., *Catal. Lett.* **25**, 271 (1994).
29. Fisher, I. A., Woo, H. C., and Bell, A. T., *Catal. Lett.* **44**, 11 (1997).
30. Kilo, M., Weigel, J., Wokaun, A., Koeppel, R. A., Stoeckli, A., and Baiker, A., *J. Mol. Catal.* **126**, 169 (1997).
31. Koeppel, R. A., Ph.D. thesis, Diss. ETH No. 9347, Swiss Federal Institute of Technology (ETH), Zürich, 1991.
32. Teichner, S. J., Nicolaon, G. A., Vicarini, M. A., and Gardes, G. E. E., *Adv. Coll. Int. Sci.* **5**, 245 (1976).
33. Pajonk, G. M., *Appl. Catal.* **72**, 217 (1991).
34. Schneider, M., Duff, D. G., Mallát, T., Wildberger, M., and Baiker, A., *J. Catal.* **147**, 500 (1994).
35. Schneider, M., Wildberger, M., Maciejewski, M., Duff, D. G., Mallát, T., and Baiker, A., *J. Catal.* **148**, 625 (1994).
36. Schneider, M., and Baiker, A., *Catal. Rev. Sci. & Eng.* **37**, 515 (1995).
37. Hüsing, N., and Schubert, U., *Angew. Chem. Int. Ed.* **37**, 22 (1998).
38. Liu, Y., Zhong, B., Peng, S., Wang, Q., Hu, T., Xie, Y. N., and Ju, X., *Catal. Today* **30**, 177 (1996).
39. Bianchi, D., Gass, J.-L., Khalfallah, M., and Teichner, S. J., *Appl. Catal. A* **101**, 297 (1993).
40. Sun, Y., and Sermon, P. A., *J. Chem. Soc., Chem. Commun.*, 1242 (1993).
41. Sun, Y., and Sermon, P. A., *Topics Catal.* **1**, 145 (1994).
42. Sun, Y., and Sermon, P. A., *Catal. Lett.* **29**, 361 (1994).
43. Stöcker, C., Schneider, M., and Baiker, A., *J. Porous Mater.* **2**, 325 (1996).
44. Lind, R. L., "CRC Handbook of Chemistry and Physics." CRC Press, Boca Raton, FL, 1993.
45. Stöcker, C., Schneider, M., and Baiker, A., *J. Porous Mater.* **2**, 171 (1995).
46. Nefedov, V. I., Gati, D., Dzhurinskii, B. F., Sergushin, N. P., and Salyn, Y. V., *Zh. Neorg. Khim.* **20**, 2307 (1975).
47. Clark, D. T., Kilcast, D., and Musgrave, W. K. R., *J. Chem. Soc., Chem. Commun.*, 516 (1971).
48. Clark, D. T., and Thomas, H. R., *J. Polym. Sci., Polym. Chem. Ed.* **16**, 791 (1978).
49. Dilks, A., *J. Polym. Sci., Polym. Chem. Ed.* **19**, 1319 (1981).
50. Shirley, D. A., *Phys. Rev. B* **5**, 4709 (1972).
51. Briggs, D., and Seah, M. P., "Practical Surface Analysis by Auger and X-ray Photoelectron Spectroscopy." Wiley, Chichester, 1983.
52. Köppel, R. A., Nickl, J., and Baiker, A., *Catal. Today* **20**, 45 (1994).

53. Evans, J. W., Wainwright, M. S., Bridgewater, A. J., and Young, D. J., *Appl. Catal.* **7**, 75 (1983).
54. Sing, K. S. W., Everett, D. H., Haul, R. A. W., Moscou, L., Pierotti, R. A., Rouquérol, J., and Siemieniewska, T., *Pure Appl. Chem.* **57**, 603 (1985).
55. Stöcker, C., and Baiker, A., *J. Non-Cryst. Solids* **223**, 165 (1998).
56. Benedetti, A., Fagherazzi, G., and Pinna, F., *J. Am. Ceram. Soc.* **72**, 467 (1989).
57. Benedetti, A., Fagherazzi, G., Pinna, F., and Polizzi, S., *J. Mater. Sci.* **25**, 1473 (1990).
58. Stöcker, C., and Baiker, A., *J. Sol-Gel Sci. Technol.* **10**, 269 (1997).
59. Bartley, G. J. J., and Burch, R., *Appl. Catal.* **43**, 141 (1988).
60. Frost, J. C., *Nature* **334**, 577 (1988).
61. Shaw, E. A., Rayment, T., Walker, A. P., Jennings, J. R., and Lambert, R. M., *J. Catal.* **126**, 219 (1990).
62. Nonneman, L. E. Y., and Ponec, V., *Catal. Lett.* **7**, 213 (1990).